Bioorganic & Medicinal Chemistry 21 (2013) 3708–3714

Contents lists available at SciVerse ScienceDirect

Bioorganic & Medicinal Chemistry

journal homepage: www.elsevier.com/locate/bmc

Synthesis and biological evaluation of ^{18}F-labled 2-phenylindole derivatives as PET imaging probes for β-amyloid plaques

Hualong Fu [a], Lihai Yu [a], Mengchao Cui [a,*], Jinming Zhang [b], Xiaojun Zhang [b], Zijing Li [a], Xuedan Wang [a], Jianhua Jia [a], Yanping Yang [a], Pingrong Yu [a], Hongmei Jia [a], Boli Liu [a,*]

[a] Key Laboratory of Radiopharmaceuticals, Ministry of Education, College of Chemistry, Beijing Normal University, Beijing 100875, PR China
[b] Department of Nuclear Medicine, Chinese PLA General Hospital, Beijing 100853, PR China

ARTICLE INFO

Article history:
Received 14 March 2013
Revised 13 April 2013
Accepted 15 April 2013
Available online 24 April 2013

Keywords:
Alzheimer's disease
β-Amyloid plaque
PET
Autoradiography
Phenylindole

ABSTRACT

A novel series of fluorinated 2-phenylindole derivatives were synthesized and evaluated as β-amyloid imaging probes for PET. The in vitro inhibition assay demonstrated that their binding affinities for $A\beta_{1-42}$ aggregates ranged from 28.4 to 1097.8 nM. One ligand was labeled with ^{18}F ([^{18}F]**1a**) for its high affinity (K_i = 28.4 nM), which was also confirmed by in vitro autoradiography experiments on brain sections of transgenic mouse (C57BL6, APPswe/PSEN1, 11 months old, male). In vivo biodistribution experiments in normal mice showed that this radiotracer displayed high initial uptake (5.82 ± 0.51% ID/g at 2 min) into and moderate washout (2.77 ± 0.31% ID/g at 60 min) from the brain. [^{18}F]**1a** could be developed as a promising new PET imaging probe for Aβ plaques although necessary modifications are still needed.

1. Introduction

Alzheimer's disease (AD) is a form of dementia which gradually worsens with the lapse of time in middle or late life. AD is related with many clinical symptoms, including cognitive decline, irreversible memory loss, disorientation, language impairment, etc. Major neuropathological features of postmortem AD brain are the presence of senile plaques and neurofibrillary tangles, which contain primarily β-amyloid (Aβ) aggregates and highly phosphorylated tau proteins, respectively.[1] Aβ hypothesis, which states that the Aβ plaques play a critical role in the deterioration of AD, is considered the most important and pivotal theory for the pathogenesis of AD.[2,3] Currently, donepezil, rivastigmine, galantamine, tacrine, and memantine are the five medications approved by the U.S. Food and Drug Administration (FDA) and used to treat moderate to severe AD patients. But these medications can only provide temporary relief from symptoms and act helplessly in halting the progression or curing AD.[4] In addition, the early diagnosis of AD keeps a difficult problem currently and needs further research urgently.

The last decade has seen a promising progress in the research field of imaging probes for Aβ plaques. Congo Red (CR) and Thioflavin-T (Th-T), which are the most common used dyes staining for Aβ plaques in human brain postmortem, have provided molecular backbones for dozens of radio-labeled Aβ imaging agents. In virtue of the high efficiency in crossing the blood–brain barrier (BBB) and selective binding to Aβ plaques, [^{11}C]PIB[5,6] ([^{11}C]6-OH-BTA-1) and [^{11}C]AZD2184[7,8] (2-(6-([^{11}C]methylamino)pyridin-3-yl)benzo[*d*]thiazol-6-ol), two analogues of Th-T with a benzothiazole ring system, have been widely used for clinical trials in AD patients or under promising commercial development, respectively. IMPY (2-(4′-dimethylamino-)phenyl-imidazo[1,2-*a*]-pyridine, K_i = 15 nM) with an imidazopyridine ring system is often used as the competing radioligand in competition binding assays when labeled by ^{125}I.[9–11] A benzofuran derivative [^{18}F]AZD4694 (2-(2-[^{18}F]fluoro-6-methylamino-pyridin-3-yl)-benzofuran-6-ol) was also evaluated as an Aβ imaging agent and displayed excellent properties.[12] Besides, our group has done some meaningful research based on the benzoxazole derivatives recently, and two ^{18}F-labeled probes with high binding affinities to Aβ aggregates and excellent in vivo brain pharmacokinetics were selected for further evaluation.[13] Benzothiophene, imidazopyridazine and benzoimidazole derivatives were also explored as Aβ imaging agents.[14–16] The Aβ imaging probes mentioned above were all belonged to the benzoheterocyclic ring system, comprising a phenyl ring fused to a five-membered heterocyclic ring (Fig. 1).[17] In addition to the Th-T scaffold, stilbene was selected as another promising scaffold for the development of Aβ imaging probes. One of these probes, [^{18}F]BAY94-9172[18,19] ((*E*)-4-(2-(4-(2-(2-(2-[^{18}F]fluoroethoxy)ethoxy)ethoxy)phenyl)vinyl]-*N*-methylaniline, K_i = 2.22 nM), was under a Phase III clinical trial currently. The styrylpyridine derivative,

* Corresponding authors. Tel./fax: +86 10 58808891.
E-mail addresses: cmc@bnu.edu.cn (M. Cui), liuboli@bnu.edu.cn (B. Liu).

0968-0896/$ - see front matter © 2013 Elsevier Ltd. All rights reserved.
http://dx.doi.org/10.1016/j.bmc.2013.04.028

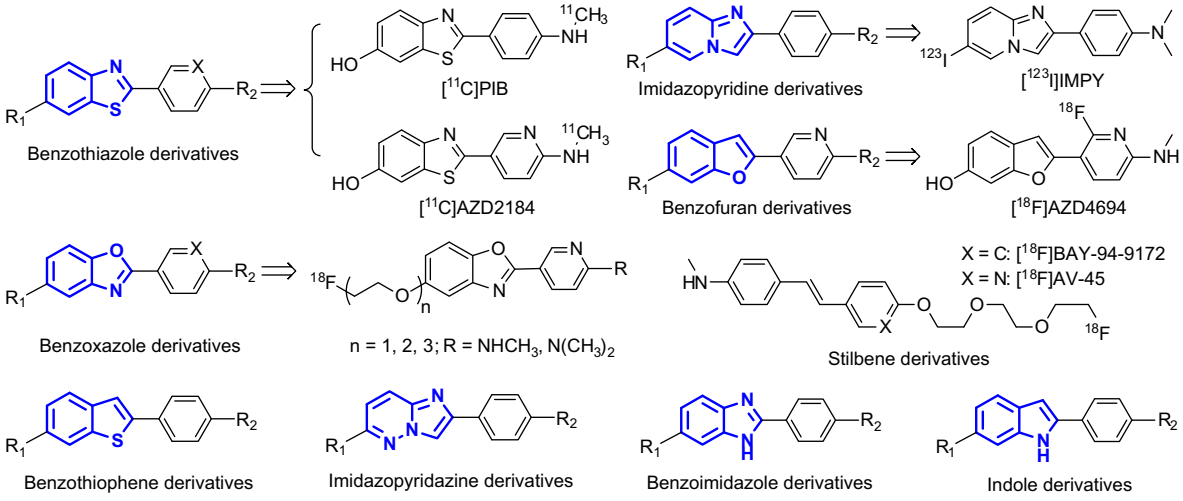

Figure 1. Structures of Aβ imaging agents based on the benzoheterocyclic and stilbene scaffolds.

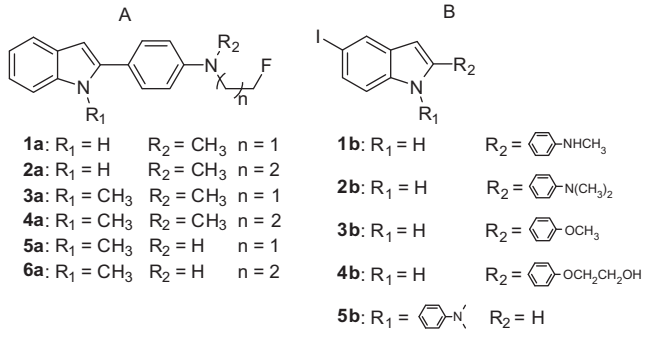

Figure 2. Chemical structures of fluorinated 2-phenyl-1*H*-indole derivatives (A) and iodinated phenylindole derivatives (B).

[^{18}F]AV-45[20] ((*E*)-4-(2-(6-(2-(2-(2-[^{18}F]fluoroethoxy) ethoxy)ethoxy)pyridin-3-yl)vinyl)-*N*-methylaniline, K_i = 2.87 nM) was the first Aβ imaging probe approved by FDA. Although great successes have been achieved in the development of Aβ imaging agents, there is still a need for novel molecular motif with better properties as Aβ probes.

Based on these facts, a novel molecular motif phenylindole, also a benzoheterocyclic ring system, was explored as Aβ imaging probes. The biological activity of indole ring is a key structural component that can be found ubiquitously in organisms, suggesting that the indole motif should have a proper biocompatibility.[21] In 2010, Watanabe et al. reported a series of ^{125}I labeled 2-phenyl-1*H*-indole and 1-phenylindole derivatives (Fig. 2B) as Aβ imaging probes.[22] 2-Phenyl-indole derivatives displayed high affinities for Aβ aggregates in binding experiments in vitro with the K_i values of 27, 4, 20, 26 nM for **1b**, **2b**, **3b**, **4b** (Fig. 2B), respectively. As a 1-phenylindole derivative, **5b** displayed a disillusionary result with the K_i value >10,000 nM, suggesting that the substituent location on the indole ring is very important for the binding affinity. Several reports have suggested the lipophilicity of probes may have a significant influence on the pharmacokinetics in vivo.[6,23] ^{125}I atoms introduced in the above radiotracers may promote the lipophilicity, which may subsequently result in the slow washout from the brain ($brain_{2\ min}/brain_{60\ min}$ ratio varies from 1.17 to 1.82 for **1b**–**4b**) and undesirable target to non-target ratio (brain/blood ratio less than 1.0) (Table 3).

Simultaneously, our group has reported a series of fluorinated 2-phenyl-1*H*-indole derivatives (Fig. 2A) as Aβ imaging probes.[24] However, ^{18}F-labeling and further biological evaluations including binding affinity were not reported. In the present study, we reported the synthesis and evaluation of these fluorinated 2-phenyl-1*H*-indole derivatives as PET radioligands for Aβ plaque imaging.

2. Results and discussion

2.1. Chemistry

The synthetic routes of ^{18}F-labeled derivatives were shown in Scheme 1 and the other fluorinated 2-phenyl-1*H*-indolederivatives except **2a** and **6a** (see Supplementary data Scheme S1) have been reported previously.[24] The skeleton of compound **1** was obtained by reacting 1-(4-methylamino-phenyl)-ethanone with phenylhydrazine in polyphosphoric acid (PPA) at 130 °C for 10 min following the classic Fischer indole synthesis method;[25] PPA acts as both catalyst and solvent in this reaction (yield, 49.0%). Compound **1a**, used as a non-radioactive ligand of [^{18}F]**1a**, was obtained by N-alkylation of **1** with 1-bromo-2-fluoro-ethane using Na_2CO_3 as base for about 24 h. Following the same reaction for **1a**, compound **2a** was synthesized by reaction of **1** with 1-fluoro-3-iodo-propane for 3 h. As iodide is a better living group compared with bromine, **2a** was made with shorter reaction time and higher yield (62.0% vs 47.0%). In order to synthesize the precursor, the hydroxyl compound **2** was prepared through N-alkylation reaction of **1** with 2-bromo-ethanol using BuOK as base and KI as catalyst (yield, 59.0%). The hydroxyl group in **2** was subsequently protected by *tert*-butyldimethylsilyl chloride (TBDMSCl) to give **3** (yield, 60.0%), and the nitrogen atom in the indole ring (indole-N) was protected by butyloxycarbonyl (BOC) group subsequently to give **4** (yield, 100.0%). After removal of the TBS-protecting group of **4** by tetrabutyl ammonium fluoride (TBAF), the free hydroxy group of **5** was converted into tosylate by reacting with *p*-toluenesulfonyl chloride (TsCl) in pyridine to give precursor **6** (yield, 59.0%) at room temperature.

2.2. Radiolabeling

[^{18}F]**1a** was prepared from the corresponding tosylate precursor **6** (Scheme 1). After the nucleophilic replacement of the tosylate leaving group by $^{18}F^-$, the N-Boc-protecting group was removed by treatment of aqueous HCl (1 M). After purification by high performance liquid chromatography (HPLC), the radiochemical purity of [^{18}F]**1a** was greater than 98%, and the specific activity was estimated approximately 136 GBq/μmol. The overall synthesis time is

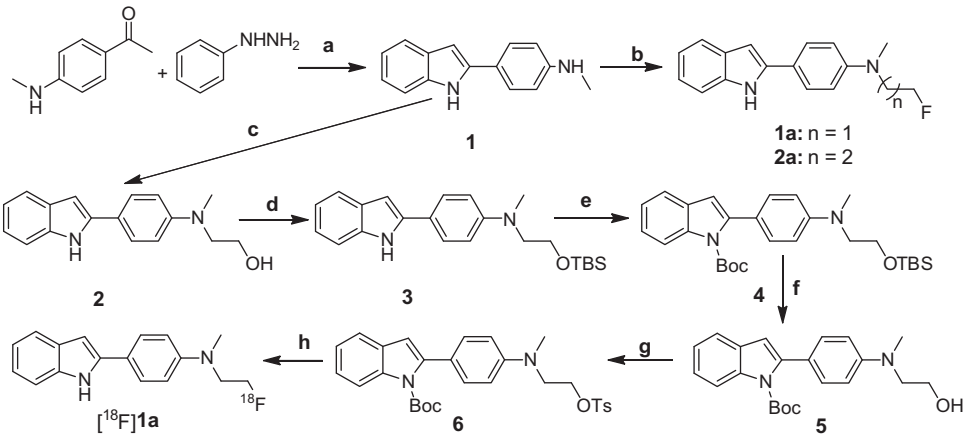

Scheme 1. Reagents and conditions: (a) PPA, 130 °C, 10 min; (b) 1-bromo-2-fluoro-ethane (for **1a**) or 1-fluoro-3-iodo-propane (for **2a**), Na_2CO_3, acetonitrile, 80 °C, 2 days (for **1a**) or 3 h (for **2a**); (c) 2-bromo–ethanol, BuOK, KI, acetonitrile, 80 °C, 3 days; (d) TBDMSCl, imidazole, CH_2Cl_2, 40 °C, 10 min; (e) $(Boc)_2O$, DMAP, CH_2Cl_2, rt, 2.5 h; (f) TBAF, THF, rt, 30 min; (g) TsCl, pyridine, rt, 3 h; (h) (1) Kryptofix-222, K_2CO_3, $^{18}F^-$, acetonitrile, 120 °C, 5 min; (2) HCl (1 M), 100 °C, 5 min; (3) $NaHCO_3$, rt.

about 60 min, and the total radiochemical yield is about 25–30% (no decay corrected, $n = 5$). The radiochemical identity of the ^{18}F-labeled ligand was verified by comparing the retention time with nonradioactive compound after co-injection (see Supplementary data Fig. S1).

2.3. In vitro binding studies

Experiments in vitro to evaluate the affinities of these fluorinated 2-phenyl-1*H*-indole derivatives for $A\beta_{1-42}$ aggregates were carried out with competition binding assays using [^{125}I]IMPY as the competing radioligand. IMPY was also measured using the same system for comparison. As shown in Table 1, **1a** and **2a** showed high affinity to $A\beta_{1-42}$ aggregates with the K_i values of 28.4 and 31.5 nM, respectively. However, **3a** (K_i = 116.8 nM), **4a** (K_i = 79.8 nM), **5a** (K_i = 1030.1 nM) and **6a** (K_i = 1097.8 nM) showed moderate or poor affinities. The comparisons of **1a** versus **2a**, **3a** versus **4a**, and **5a** versus **6a** showed the length of the fluorinated alkyl chain has slight influence on the affinity. On the contrary, the methylation of the indole-N gave negative effects on the affinity of the probes, approving by the higher K_i values of **3a**, **4a**, **5a**, and **6a** compared with those of **1a** and **2a**. This is in accordance with the results of 5-iodinated-1-phenylindole derivative.[22] Since the tertiary *N,N*-dialkylamino group can bring about a positive promotion to the affinity of Aβ probes,[26] **5a** and **6a**, lack of this important group together with the single methyl substitutions at the indole-N, displayed poor affinity to $A\beta_{1-42}$ aggregates. On the basis of the high binding affinity to $A\beta_{1-42}$ aggregates, **1a** was selected for ^{18}F labeling and further evaluation.

Table 1
Inhibition constants (K_i) for binding of fluorinated 2-phenyl-1*H*-indole derivatives to $A\beta_{1-42}$ aggregates

Compd	$K_i \pm$ SEM (nM) [a]
1a	28.4 ± 7.4
2a	31.5 ± 11.3
3a	116.8 ± 35.9
4a	79.7 ± 31.2
5a	1030.1 ± 375.2
6a	1097.8 ± 171.6
IMPY	10.5 ± 1.0

[a] The K_i values were determined in three independent experiments ($n = 3$).

2.4. In vitro autoradiography studies

To confirm the specific and high binding affinity of [^{18}F]**1a** to Aβ plaques, in vitro autoradiography experiments were performed on the brain sections of Tg mouse (C57BL6, APPswe/PSEN1, 11 months old, male) and age-matched wild-type mouse (C57BL6, 11 months old, male). As shown in Figure 3, the distinctive labeling of Aβ plaques in the hippocampus and cortical regions of the Tg mouse brain section was observed (Fig. 3, A and C), while wild-type mouse brain displayed no such labeling (Fig. 3, G). The positions (or patterns) of the labeled Aβ plaques with [^{18}F]**1a** were also visible by co-staining the same sections with thioflavin-S (Fig. 3, B, E and F), confirming that there is a good correlation between the two different techniques in identifying Aβ plaques. In addition, some Aβ plaques in the cerebellum region can be clearly observed in this kind of transgenic mouse model of AD (Fig. 3, D and F), which was in accord with the results reported previously.[27]

2.5. In vivo biodistribution studies

To evaluate the uptake and washout kinetics of [^{18}F]**1a** in brain, a biodistribution experiment was performed in normal ICR mice (5 weeks, male) (Table 2). Since a log*D* value in the range of 0.9–2.5 guarantees a radiotracer free penetration across the blood–brain barrier,[23] a higher log*D* value (3.61) for [^{18}F]**1a** was important for the brain penetration and may result in high brain uptake directly. [^{18}F]**1a** displayed high initial brain uptake (5.82% ID/g) at 2 min post-injection and the radioactivity in the brain displayed moderate washout rate (2.77% ID/g at 60 min) with a $brain_{2\ min}/brain_{60\ min}$ ratio of 2.10. In addition, a preferable signal to noise ratio was achieved with the $brain_{2\ min}/blood_{2\ min}$ ratio of 1.72. Those values are better compared with those of radioiodinated 2-phenyl-1*H*-indole derivatives reported previously (Table 3).[22] However, in vivo defluorination likely occurs with [^{18}F]**1a**, because substantial bone uptake of radioactivity was increased with time (2.05% ID/g at 2 min and 9.71% ID/g at 1 h) after the administration of [^{18}F]**1a** to normal mice. This observation was in accord with the ^{18}F-labeled IMPY derivatives, which may due to the in vivo N-dealkylation of the *N*-2-[^{18}F]fluoroethyl group.[28] Furthermore, [^{18}F]**1a** distributed to several other organs simultaneously. The radiotracer distributed to liver and kidneys with a high initial uptake (10.47 ± 1.35 and 9.66 ± 1.30% ID/g at 2 min, respectively) and then was washed out with a moderate rate (4.15 ± 0.27 and 3.54 ± 0.33% ID/g at 60 min, respectively). But the radioactivity was observed to accumulate within the intestines over time (the uptake ranged from 6.50 ± 1.04% ID/g at 2 min to 11.04 ± 1.54% ID/g at 60 min).

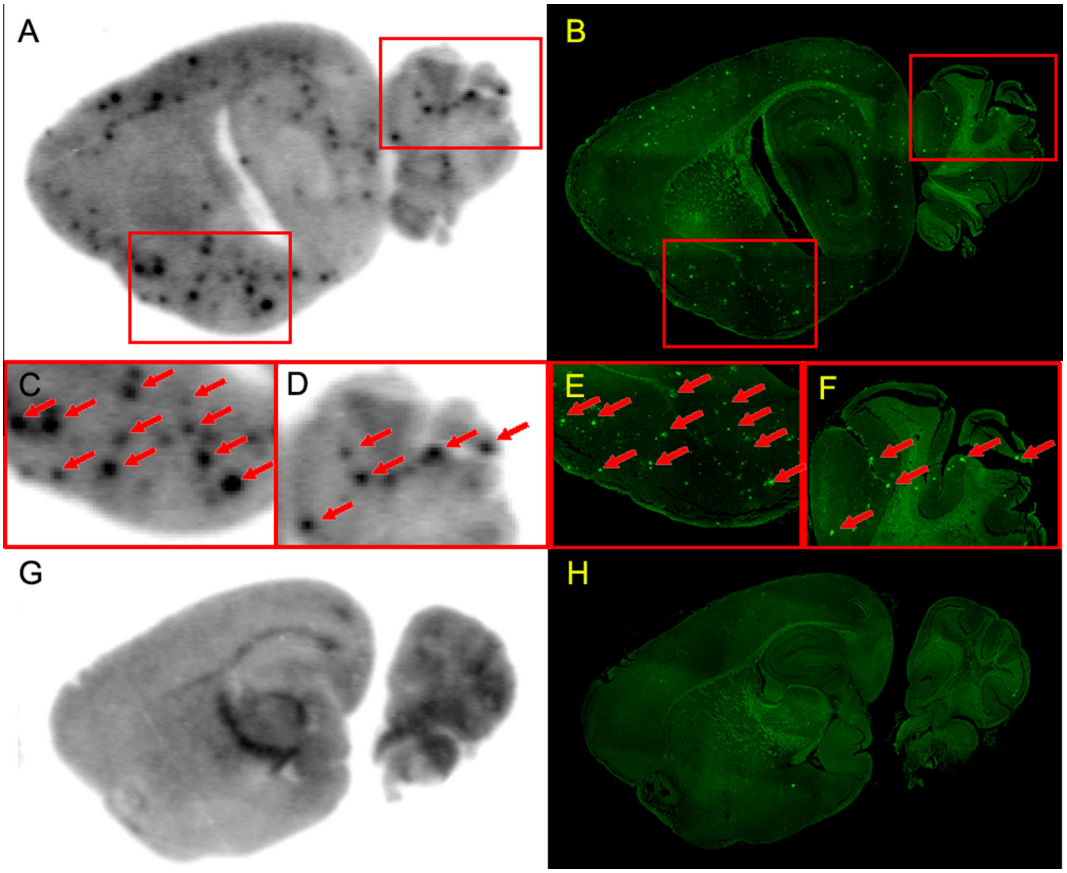

Figure 3. Autoradiography of [^{18}F]**1a** ex vivo using Tg model mouse (C57BL6, APPswe/PSEN1, 11 months old, male) (A, C, D) and wild-type controls (C57BL6, 11 months old) (G). Plaques were also confirmed by the staining of the same sections with thioflavin-S (B, E, F and H).

Table 2
Biodistribution in normal ICR mice after intravenous injection of the [^{18}F]**1a** [a]

Organ	Time after injection (min)			
	2	10	30	60
[^{18}F]**1a** (log*D* = 3.61)				
Blood	3.38 ± 0.20	3.81 ± 0.44	4.21 ± 0.09	4.37 ± 0.24
Brain	5.82 ± 0.51	5.07 ± 0.18	3.41 ± 0.10	2.77 ± 0.31
Heart	6.76 ± 0.62	4.95 ± 0.24	3.71 ± 0.06	3.81 ± 0.59
Liver	10.47 ± 1.35	8.38 ± 0.79	4.86 ± 0.37	4.15 ± 0.27
Spleen	2.73 ± 0.65	3.97 ± 0.56	3.23 ± 0.12	2.71 ± 0.46
Lung	6.57 ± 1.33	5.81 ± 1.07	4.27 ± 0.19	3.57 ± 0.50
Kidney	9.66 ± 1.30	5.62 ± 0.34	4.17 ± 0.30	3.54 ± 0.33
Bone	2.05 ± 0.39	4.13 ± 1.27	5.95 ± 0.95	9.71 ± 1.00
Stomach[b]	1.38 ± 0.16	1.54 ± 0.11	1.43 ± 0.25	1.09 ± 0.17
Intestine[b]	6.50 ± 1.04	9.06 ± 0.54	9.00 ± 1.52	11.04 ± 1.54

[a] Expressed as% injected dose per gram. Average for five mice ± standard deviation.
[b] Expressed as% injected dose per organ.

Table 3
Comparison of brain kinetics between [^{18}F]**1a** and radio-iodonated tracers[a]

Compd	Brain uptake at 2 min[b]	$Brain_{2\ min}/brain_{60\ min}$ ratio	$Brain_{2\ min}/blood_{2\ min}$ ratio
[^{125}I]**1b**	1.10 ± 0.27	1.33	0.29
[^{125}I]**2b**	1.19 ± 0.34	1.68	0.19
[^{125}I]**3b**	2.11 ± 0.69	1.82	0.59
[^{125}I]**4b**	2.13 ± 0.54	1.17	0.52
[^{18}F]**1a**	5.82 ± 0.51	2.10	1.72

[a] The data for [^{125}I]**1b**–**4b** are original from Ref. 22.
[b] Expressed as% injected dose per gram.

3. Conclusions

In conclusion, on the basis of our previous work, we evaluated a series of fluorinated 2-phenyl-1*H*-indole derivatives (**1a**, **2a**, **3a**, **4a**, **5a**, **6a**) as Aβ imaging probe compounds. **1a** and **2a** displayed high affinity to Aβ aggregates in binding experiments in vitro. In addition, [^{18}F]**1a** can clearly and selectively bind to Aβ plaques on Tg mouse brain sections, which confirmed its affinity to Aβ aggregates in vitro. The in vivo biodistribution experiments in normal mice indicated that [^{18}F]**1a** displayed excellent uptake into and moderate washout from the brain. However, [^{18}F]**1a** was unstable for in vivo defluorination, thus additional structure modifications of these fluorinated 2-phenyl-1*H*-indole derivatives were needed, and may bring potential Aβ imaging probes for PET.

4. Experimental section

4.1. General remarks

All reagents used in the synthesis were commercial products and were used without further purification unless otherwise indicated. The ^{1}H NMR spectra were obtained at 400 MHz on Bruker spectrometer in $CDCl_3$ solutions at room temperature with TMS as an internal standard. Chemical shifts were reported as δ values relative to the internal TMS. Coupling constants were reported in Hertz. Multiplicity is defined by s (singlet), d (doublet), t (triplet), and m (multiplet). Mass spectra were acquired under Surveyor MSQ Plus (ESI) instrument. Reactions were monitored by TLC (Silica gel 60 F_{254} aluminum sheets, Merck) and compounds were visualized by illumination with a short wavelength UV lamp

(λ = 254 nm or 365 nm). Column chromatography purification were performed on silica gel (54–74 μm) from Qingdao Haiyang Chemical Co., Ltd. Radiochemical purity was determined by HPLC performed on a Shimadzu system SCL-20 AVP equipped with a SPD-20A UV detector (λ = 254 nm) and Bioscan Flow Count 3200 NaI/PMT γ-radiation scintillation detector. HPLC separations were achieved on a Venusil MP C18 reverse phase column (Agela Technologies, 5 μm, 10 mm × 250 mm) eluted with a binary gradient system at a flow rate of 4.0 mL/min and HPLC analysis were achieved on a Venusil MP C18 reverse phase column (Agela Technologies, 5 μm, 4.6 mm × 250 mm) eluted with a binary gradient system at a flow rate of 1.0 mL/min. Mobile phase A was water while mobile phase B was acetonitrile. The purity of the synthesized key compounds was determined using analytical HPLC and was found to be more than 95%. Fluorescent observation was performed on the Observer Z1 (Zeiss, Germany) equipped with GFP filter set (excitation, 505 nm). Normal ICR mice (five weeks, male) were used for biodistribution experiments. Transgenic mice (C57BL6, APPswe/PSEN1, 11 months old, male), used as an Alzheimer's model, were purchased from the Institute of Laboratory Animal Science, Chinese Academy of Medical Sciences. All protocols requiring the use of mice were approved by the animal care committee of Beijing Normal University.

4.1.1. 4-[(1*H*-Indol-2-yl)-phenyl]-methyl-amine (1)

1-(4-Methylamino-phenyl)-ethanone (937 mg, 6.3 mmol) and phenyl-hydrazine (750 mg, 7.0 mmol) were mixed in jelled polyphosphoric acid (PPA, 15.0 g). The reaction mixture was kept at 130 °C for 10 min. Ice water (50 mL) was added and the mixture was neutralized by ammonia water. The gray precipitate was collected by filtration, washed with hot water and then dried at 80 °C. The residue was purified by flash column chromatography to give compound **1** as a white solid (684 mg, 49.0%). ^{1}H NMR (400 MHz, $CDCl_3$) δ: 2.88 (s, 3H), 6.64 (s, 1H), 6.66 (d, J = 8.8 Hz, 2H), 7.07–7.15 (m, 2H), 7.35 (d, J = 8.0 Hz, 1H), 7.49 (d, J = 8.6 Hz, 2H), 7.58 (d, J = 7.7 Hz, 1H), 8.19 (s, 1H). MS (ESI): m/z calcd for $C_{15}H_{14}N_2$ 222.1, found 223.1 $(M+H)^+$.

4.1.2. 4-(1*H*-Indol-2-yl)-*N*-(2-fluoroethyl)-*N*-methylbenzenamine (1a)

A solution of compound **1** (101 mg, 0.5 mmol), 1-bromo-2-fluoroethane (437 mg, 2.6 mmol) and Na_2CO_3 (0.22 g, 2 mmol) in acetonitrile (10 mL) was stirred at 80 °C for 2 days. Water was added and the mixture was extract with ethyl acetate (3 × 50 mL). The organic layer was washed with saturated brine (50 mL) and dried over anhydrous magnesium sulfate. After the ethyl acetate was removed in vacuum, the residue was purified by flash column chromatography to give compound **1a** as a yellowish solid (58 mg, 47.0%). ^{1}H NMR (400 MHz, $CDCl_3$) δ: 3.08 (s, 3H), 3.70 (dt, J = 24.4 Hz, 4.9 Hz, 2H), 4.65 (dt, J = 47.1 Hz, 5.1 Hz, 2H), 6.67 (s, 1H), 6.82 (d, J = 8.2 Hz, 2H), 7.09 (dd, J = 7.2 Hz, 7.1 Hz, 1H), 7.14 (dd, J = 7.2 Hz, 7.0 Hz, 1H) 7.37 (d, J = 7.9 Hz, 1H), 7.56 (d, J = 8.8 Hz, 2H), 7.58 (d, J = 8.0 Hz), 8.24 (s, 1H). MS (ESI): m/z calcd for $C_{17}H_{17}N_2F$ 269.2; found 269.1 (M^+).

4.1.3. (3-Fluoro-propyl)-[4-(1*H*-indol-2-yl)-phenyl]-amine (2a)

The same reaction as described above to prepare **1a** was used, and a yellowish solid **2a** was obtained (79 mg, 62.0%). ^{1}H NMR (300 MHz, $CDCl_3$) δ: 1.97 (m, 1H), 2.04 (m, 1H), 3.02 (s, 3H), 3.55 (t, J = 5.4 Hz, 2H), 4.48 (t, J = 4.2 Hz, 1H), 4.60 (t, J = 4.2 Hz, 1H), 6.67 (s, 1H), 6.78 (d, J = 6.6 Hz, 2H), 7.10 (t, J = 5.4 Hz, 1H), 7.15 (t, J = 5.4 Hz, 1H), 7.37 (d, J = 6.3 Hz, 1H), 7.54 (d, J = 6.9 Hz, 2H), 7.59 (d, J = 5.7 Hz, 1H), 8.20 (b, 2H). MS (ESI): m/z calcd for $C_{19}H_{19}N_2F$ 282.2; found 283.0 (M^+).

4.1.4. 2-[4-(1*H*-Indol-2-yl)-phenyl]-methyl-amino-ethanol (2)

To the solution of compound **1** (191 mg, 0.9 mmol) and 2-bromo-ethanol (513 mg, 4.1 mmol) in acetonitrile (15 mL) was added BuOK (223 mg, 2.0 mmol) and KI (catalytic amount). The reaction mixture was stirred at 80 °C for 3 days. Water was added and the mixture was extract with ethyl acetate (3 × 50 mL). In the following, the organic phase was washed with water (100 mL) and saturated brine (100 mL), and then dried over anhydrous magnesium sulfate. Remove the solvent in vacuum and the residue was purified by flash column chromatography to give compound **2** as a yellow solid (55 mg, 59.0%). ^{1}H NMR (400 MHz, $CDCl_3$) δ: 3.03 (s, 3H), 3.53 (t, J = 5.6 Hz, 2H), 3.85 (t, J = 5.6 Hz, 2H), 6.67 (d, J = 1.2 Hz, 1H), 6.87 (d, J = 8.6 Hz, 2H), 7.09 (dd, J = 7.1 Hz, 6.9 Hz, 1H), 7.14 (dd, J = 7.7 Hz, 6.4 Hz, 1H), 7.37 (d, J = 7.8 Hz, 1H), 7.54 (d, J = 8.8 Hz, 2H), 7.58 (d, J = 7.7 Hz, 1H), 8.25 (s, 1H). MS (ESI): m/z calcd for $C_{17}H_{18}N_2O$ 266.1, found 267.2 $(M+H)^+$.

4.1.5. 2-[(*tert*-Butyl-dimethyl-silanyloxy)-ethyl]-[4-(1*H*-indol-2-yl)-phenyl]-methyl-amine (3)

To the solution of compound **2** (45 mg, 0.2 mmol) and TBDMSCl (92 mg, 0.6 mmol) in CH_2Cl_2 (10 mL) was added imidazole (35 mg, 0.5 mmol). The mixture was stirred for 10 min at 40 °C. Solvent was removed in vacuum and the residue was purified by flash column chromatography to give compound **3** as a white solid (39 mg, 60.0%). ^{1}H NMR (400 MHz, $CDCl_3$) δ: 0.03 (s, 6H), 0.85 (s, 9H), 3.02 (s, 3H), 3.49 (t, J = 6.0 Hz, 2H), 3.78 (t, J = 5.9 Hz, 2H), 6.63 (s, 1H), 6.76 (s, 2H), 7.05 (dd, J = 7.0 Hz, 6.8 Hz, 1H), 7.10 (dd, J = 6.9 Hz, 7.1 Hz, 1H), 7.33 (d, J = 7.8 Hz, 1H), 7.50 (d, J = 8.6 Hz, 2H), 7.55 (d, J = 7.6 Hz, 1H), 8.21 (s, 1H). MS (ESI): m/z calcd for $C_{23}H_{32}N_2OSi$ 380.2, found 380.5 (M^+).

4.1.6. 2-(4-{[2-(*tert*-Butyl-dimethyl-silanyloxy)-ethyl]-methyl-amino}-phenyl)-indole-1-carboxylic acid *tert*-butyl ester (4)

To the solution of compound **3** (38 mg, 0.1 mmol) and $(Boc)_2O$ (170 mg, 0.8 mmol) in CH_2Cl_2 (10 mL) was added DMAP (catalytic amount). The reaction mixture was stirred at room temperature for 2.5 h. Solvent was removed in vacuum and the residue was purified by flash column chromatography to give compound **4** as a yellowish oily liquid (56 mg, 100.0%). ^{1}H NMR (400 MHz, $CDCl_3$) δ: 0.04 (s, 6H), 0.89 (s, 9H), 1.39 (s, 9H), 3.05 (s, 3H), 3.51 (t, J = 6.0 Hz, 2H), 3.81 (s, 2H), 6.48 (s, 1H), 6.76 (s, 2H), 7.20–7.28 (m, 4H), 7.52 (d, J = 7.3 Hz, 1H), 8.15 (d, J = 8.2 Hz, 1H). MS (ESI): m/z calcd for $C_{28}H_{40}N_2O_3Si$ 480.3, found 481.4 $(M+H)^+$.

4.1.7. 2-{4-[(2-Hydroxy-ethyl)-methyl-amino]-phenyl}-indole-1-carboxylic acid *tert*-butyl ester (5)

To the solution of compound **4** (56 mg, 0.1 mmol) in THF (10 mL) was added TBAF (2 mL, 1 M in THF, 2 mmol). The reaction mixture was stirred for 30 min at room temperature, and then oily liquid was given after the solvent was removed in vacuum. Wash the oily liquid with water (50 mL) and extract the mixture with CH_2Cl_2 (3 × 25 mL); in the following, the organic phase was washed with water (3 × 50 mL) and dried over anhydrous magnesium sulfate. Solvent was removed in vacuum and the residue was purified by flash column chromatography to give compound **5** as a yellowish oily liquid (33 mg, 89.0%). ^{1}H NMR (400 MHz, $CDCl_3$) δ: 1.40 (s, 9H), 3.03 (s, 3H), 3.53 (s, 2H), 3.85 (s, 2H), 6.49 (s, 1H), 6.85 (d, J = 8.2 Hz, 2H), 7.20–7.32 (m, 4H), 7.52 (d, J = 7.4 Hz, 1H), 8.14 (d, J = 8.2 Hz, 1H). MS (ESI): m/z calcd for $C_{22}H_{26}N_2O_3$ 366.2, found 367.2 $(M+H)^+$.

4.1.8. 2-(4-{Methyl-[2-(toluene-4-sulfonyloxy)-ethyl]-amino}-phenyl)-indole-1-carboxylic acid *tert*-butyl ester (6)

To the solution of compound **5** (33 mg, 0.09 mmol) in anhydrous pyridine (1 mL) was added TsCl (43 mg, 0.2 mmol) after it cooled to 0 °C in ice-water. The reaction mixture was stirred for

3 h with the temperature rising slowly from 0 °C to room temperature. Water was added and the water phase was extract with ethyl acetate (3 × 50 mL). In the following, wash the combined organic phase with water (100 mL) and dry over anhydrous magnesium sulfate, then remove the solvent in vacuum. The residue was purified by flash column chromatography to give compound **6** as a yellowish oily liquid (27 mg, 59.0%). ^{1}H NMR (400 MHz, $CDCl_3$) δ: 1.39 (s, 9H), 2.41 (s, 3H), 2.94 (s, 3H), 3.65 (t, J = 6.0 Hz, 2H), 4.19 (t, J = 6.0 Hz, 2H), 6.47 (s, 1H), 6.61 (d, J = 8.8 Hz, 2H), 7.20–7.31 (m, 6H), 7.52 (d, J = 7.3 Hz, 1H), 7.75 (d, J = 8.3 Hz, 2H), 8.14 (d, J = 8.2 Hz, 1H). MS (ESI): m/z calcd for $C_{29}H_{32}N_2O_5S$ 520.2, found 521.2 $(M+H)^+$.

4.2. Radiolabeling

[^{18}F]Fluoride on the QMA cartridge was eluted into a 10 mL reaction vial with 1 mL of Kryptofix$_{222}$/K_2CO_3 solution (13 mg of Kryptofix$_{222}$ and 1.1 mg of K_2CO_3 in CH_3CN/H_2O, 4/1, v/v). The solvent was removed by continuously blowing of nitrogen at 120 °C. Subsequently, the residue was azeotropically dried with 1 mL of anhydrous acetonitrile three times at 120 °C under a stream of nitrogen gas. Tosylate precursor **6** (4–5 mg) was added to the reaction vessel after being dissolved in 1 mL anhydrous acetonitrile. The reaction mixture was heated to 100 °C and kept for 5 min. A solution of HCl (200 μL, 1 M) was added to the mixture after it cooled down to room temperature, and then keep the reaction vial at 100 °C for additional 5 min. Subsequently, the reaction mixture was neutralized with anhydrous sodium hydrogen carbonate and then 10 mL of water was added. The mixture flowed past a preconditioned Sep-Pak C18 (Waters) cartridge and wash the cartridge with 20 mL of water afterwards to remove the inorganic salt. The labeled compound [^{18}F]**1a** was eluted with 1.5 mL of acetonitrile and then the solvent was removed with a stream of nitrogen. The residue was redissolved in acetonitrile and then purified with HPLC (Agela Technologies, 5 μm, 10 mm × 250 mm, CH_3CN/water = 7/3; flow rate = 4.0 mL/min). The retention time of [^{18}F]**1a** was 9.57 min in this HPLC system. The specific activity was estimated by comparing the UV peak intensity of purified ^{18}F-labeled compounds with reference nonradioactive compounds.

4.3. Binding assays in vitro using Aβ_{1-42} aggregates

The affinity of these fluorinated 2-phenylindoles derivatives were first evaluated by in vitro competitive binding assays with [^{125}I]IMPY for Aβ_{1-42} aggregates in solution. The radio-ligand [^{125}I]IMPY was prepared according to procedures described previously.[11] After HPLC purification, the radiochemical purity of [^{125}I]IMPY was greater than 95%. A solid form of Aβ_{42} was purchased from Osaka Peptide Institute and the Aβ_{1-42} aggregates were prepared following the procedures described previously.[22] The inhibition experiments were carried out in 12 × 75 mm borosilicate glass tubes with the reaction mixture containing 100 μL of aggregated Aβ_{1-42} fibrils, 100 μL of radioligand [^{125}I]IMPY (100,000 cpm/100 μL), 100 μL of test compound (10^{-4} to $10^{-8.5}$ M in ethanol) and 700 μL of 0.05% bovine serum albumin solution in a total volume of 1 mL. The mixture was incubated at room temperature for 3 h before it was filtered through Whatman GF/B filters using a Brandel Mp-48T cell harvester. Filters containing the bound [^{125}I]IMPY were measured by gamma counter (WALLAC/Wizard 1470, USA) with 70% counting efficiency. The half maximal inhibitory concentration (IC_{50}) was determined from displacement curves of three independent experiments using GraphPad Prism 4.0 and the inhibition constant (K_i) was calculated using the Cheng–Prusoff equation:[29] $K_i = IC_{50}/(1 + [L]/K_d)$, where [L] is the concentration of [^{125}I]IMPY used in the assay and K_d is the dissociation constant of IMPY.[9]

4.4. Determination of the partition coefficient

The determination of partition coefficients of radiofluorinated tracers was performed using the method previously reported.[30] A solution of ^{18}F-labeled tracer (1110 kBq) was added to a premixed suspension containing 3.0 g n-octanol and 3.0 g PBS (0.05 M, pH = 7.4) in a test tube, vortexed for 3 min at room temperature, and then centrifuged for 5 min at 3000 rpm. Two aliquots from the n-octanol (50 μL) and water (500 μL) layers were measured. The partition coefficient was expressed as the logarithm of the ratio of the count per gram from n-octanol versus PBS. Samples from the n-octanol layer were repartitioned until the partition coefficient values tend to stabilization. The measurement was conducted in triplicate and repeated five times.

4.5. Biodistribution studies

The biodistribution experiments were performed in normal ICR mice (5 weeks, male) and approved by the Animal Care Committee of Beijing Normal University. A saline solution containing the [^{18}F]**1a** (740–1110 kBq/mL) with 10% EtOH was intravenously injected into the tail, and the mice (n = 5 for each time point) were sacrificed at 2, 10, 30 and 60 min post injection. The organs of interest were removed, weighed and counted with an automatic gamma counter. Data are expressed as the percent injected dose per gram of tissues (% ID/g).

4.6. In vitro autoradiography using brain sections from Tg mouse

Paraffin-embedded Tg mouse and a wild type mouse brain sections were treated following the previous method reported.[13] The brain sections were incubated with [^{18}F]**1a** (185–370 kBq) for 1 h at room temperature. Finally, the sections were washed with 40% EtOH. After drying, the ^{18}F-labeled sections were exposed to an imaging plate (PerkinElmer, USA) for 1 h. Autoradiographic images were obtained using a scanner system (Cyclone, Packard). The presence and location of plaques were confirmed with fluorescent staining using thioflavin-S (0.125%) on the same brain sections.

Acknowledgments

The authors thank Dr. Jin Liu (College of Life Science, Beijing Normal University) for assistance in the in vitro neuropathological staining. This work was funded by National Natural Science Foundation of China (No. 21201019) and Doctoral Fund of Ministry of Education of China (No. 20120003120013) and Fundamental Research Funds for the Central Universities (No. 2012LYB19).

Supplementary data

Supplementary data associated with this article can be found, in the online version, at http://dx.doi.org/10.1016/j.bmc.2013.04.028.

References and notes

1. Jucker, M.; Walker, L. C. *Ann. Neurol.* **2011**, *70*, 532.
2. Hardy, J.; Selkoe, D. J. *Science* **2002**, *297*, 353.
3. Hardy, J. A.; Higgins, G. A. *Science* **1992**, *256*, 184.
4. Kung, H. F. *ACS Med. Chem. Lett.* **2012**, *3*, 265.
5. Klunk, W. E.; Engler, H.; Nordberg, A.; Wang, Y.; Blomqvist, G.; Holt, D. P.; Bergström, M.; Savitcheva, I.; Huang, G.-F.; Estrada, S.; Ausén, B.; Debnath, M. L.; Barletta, J.; Price, J. C.; Sandell, J.; Lopresti, B. J.; Wall, A.; Koivisto, P.; Antoni, G.; Mathis, C. A.; Långström, B. *Ann. Neurol.* **2004**, *55*, 306.
6. Mathis, C. A.; Wang, Y.; Holt, D. P.; Huang, G.-F.; Debnath, M. L.; Klunk, W. E. *J. Med. Chem.* **2003**, *46*, 2740.
7. Johnson, A. E.; Jeppsson, F.; Sandell, J.; Wensbo, D.; Neelissen, J. A.; Jureus, A.; Strom, P.; Norman, H.; Farde, L.; Svensson, S. P. *J. Neurochem.* **2009**, *108*, 1177.

8. Nyberg, S.; Jonhagen, M. E.; Cselenyi, Z.; Halldin, C.; Julin, P.; Olsson, H.; Freund-Levi, Y.; Andersson, J.; Varnas, K.; Svensson, S.; Farde, L. *Eur. J. Nucl. Med. Mol. Imaging* **1859**, *2009*, 36.
9. Kung, M.-P.; Hou, C.; Zhuang, Z.-P.; Zhang, B.; Skovronsky, D.; Trojanowski, J. Q.; Lee, V. M. Y.; Kung, H. F. *Brain Res.* **2002**, *956*, 202.
10. Newberg, A. B.; Wintering, N. A.; Plössl, K.; Hochold, J.; Stabin, M. G.; Watson, M.; Skovronsky, D.; Clark, C. M.; Kung, M.-P.; Kung, H. F. *J. Nucl. Med.* **2006**, *47*, 748.
11. Zhuang, Z.-P.; Kung, M.-P.; Wilson, A.; Lee, C.-W.; Plössl, K.; Hou, C.; Holtzman, D. M.; Kung, H. F. *J. Med. Chem.* **2002**, *46*, 237.
12. Schou, M.; Peter, J.; Varnas, K.; Anders, J.; Sandell, J.; Cselenyi, Z.; Swahn, B. M.; Svensson, S.; Lindstrom-Boo, E.; Farde, L.; Halldin, C. *J. Labelled Compd. Radiopharm.* **2011**, *54*, S41.
13. Cui, M.; Wang, X.; Yu, P.; Zhang, J.; Li, Z.; Zhang, X.; Yang, Y.; Ono, M.; Jia, H.; Saji, H.; Liu, B. *J. Med. Chem.* **2012**, *55*, 9283.
14. Chang, Y. S.; Jeong, J. M.; Lee, Y.-S.; Kim, H. W.; Ganesha, R. B.; Kim, Y. J.; Lee, D. S.; Chung, J.-K.; Lee, M. C. *Nucl. Med. Biol.* **2006**, *33*, 811.
15. Cui, M.; Ono, M.; Kimura, H.; Kawashima, H.; Liu, B. L.; Saji, H. *Nucl. Med. Biol.* **2011**, *38*, 313.
16. Zeng, F.; Alagille, D.; Tamagnan, G. D.; Ciliax, B. J.; Levey, A. I.; Goodman, M. M. *ACS Med. Chem. Lett.* **2010**, *1*, 80.
17. Cui, M.; Ono, M.; Kimura, H.; Liu, B.; Saji, H. *Bioorg. Med. Chem. Lett.* **2011**, *21*, 4193.
18. Rowe, C. C.; Ackerman, U.; Browne, W.; Mulligan, R.; Pike, K. L.; O'Keefe, G.; Tochon-Danguy, H.; Chan, G.; Berlangieri, S. U.; Jones, G.; Dickinson-Rowe, K. L.; Kung, H. P.; Zhang, W.; Kung, M. P.; Skovronsky, D.; Dyrks, T.; Hall, G.; Krause, S.; Friebe, M.; Lehman, L.; Lindemann, S.; Dinkelborg, L. M.; Masters, C. L.; Villemagne, V. L. *Lancet Neurol.* **2008**, *7*, 129.
19. Zhang, W.; Oya, S.; Kung, M. P.; Hou, C.; Maier, D. L.; Kung, H. F. *J. Med. Chem.* **2005**, *48*, 5980.
20. Zhang, W.; Kung, M. P.; Oya, S.; Hou, C.; Kung, H. F. *Nucl. Med. Biol.* **2007**, *34*, 89.
21. Wei, Y.; Deb, I.; Yoshikai, N. *J. Am. Chem. Soc.* **2012**, *134*, 9098.
22. Watanabe, H.; Ono, M.; Haratake, M.; Kobashi, N.; Saji, H.; Nakayama, M. *Bioorg. Med. Chem.* **2010**, *18*, 4740.
23. Dischino, D. D.; Welch, M. J.; Kilbourn, M. R.; Raichle, M. E. *J. Nucl. Med.* **1983**, *24*, 1030.
24. Yu, L. H.; Scheunemann, M.; Deuther-Conrad, W.; Hiller, A.; Fischer, S.; Sorger, D.; Sabri, O.; Jia, H. M.; Steinbach, J.; Brust, P.; Liu, B. L. *Bull. Korean Chem. Soc.* **2010**, *31*, 177.
25. Robinson, B. *Chem. Rev.* **1963**, *63*, 373.
26. Ono, M.; Cheng, Y.; Kimura, H.; Cui, M.; Kagawa, S.; Nishii, R.; Saji, H. *J. Med. Chem.* **2011**, *54*, 2971.
27. Kung, M. P.; Hou, C.; Zhuang, Z. P.; Cross, A. J.; Maier, D. L.; Kung, H. F. *Eur. J. Nucl. Med. Mol. Imaging* **2004**, *31*, 1136.
28. Cai, L.; Chin, F. T.; Pike, V. W.; Toyama, H.; Liow, J.-S.; Zoghbi, S. S.; Modell, K.; Briard, E.; Shetty, H. U.; Sinclair, K.; Donohue, S.; Tipre, D.; Kung, M.-P.; Dagostin, C.; Widdowson, D. A.; Green, M.; Gao, W.; Herman, M. M.; Ichise, M.; Innis, R. B. *J. Med. Chem.* **2004**, *47*, 2208.
29. Cheng, Y.; Prusoff, W. H. *Biochem. Pharmacol.* **1973**, *22*, 3099.
30. Cui, M.; Ono, M.; Kimura, H.; Ueda, M.; Nakamoto, Y.; Togashi, K.; Okamoto, Y.; Ihara, M.; Takahashi, R.; Liu, B.; Saji, H. *J. Med. Chem.* **2012**, *55*, 9136.